AD

AD-E402 700

Technical Report ARAED-TR-95018

INFLUENCE OF ADDED GRAPHITE ON THE MECHANICAL STRENGTH OF PRESSED PLASTIC BONDED EXPLOSIVES

Donald A. Wiegand

January 1996

U.S. ARMY ARMAMENT RESEARCH, DEVELOPMENT AND ENGINEERING CENTER

Armament Engineering Directorate

Picatinny Arsenal, New Jersey

US ARMY
TANK AUTOMOTIVE AND
ARMAMENTS COMMAND
ARMAMENT RDE CENTER

19960201 063

REPORT DOCUMENTATION PAGE	Form Approved OMB No. 0704-0188

Public reporting burden for this collection of information is estimated to average 1 hour per response, including the time for reviewing instructions, searching existing data sources, gathering and maintaining the data needed, and completing and reviewing the collection of information. Send comments regarding this burden estimate or any other aspect of this collection of information, including suggestions for reducing this burden, to Washington Headquarters Services, Directorate for Information Operation and Reports, 1215 Jefferson Davis Highway, Suite 1204, Arlington, VA 22202-4302, and to the Office of Management and Budget, Paperwork Reduction Project (0704-0188), Washington, DC 20503.

1. AGENCY USE ONLY (Leave blank)	2. REPORT DATE January 1996	3. REPORT TYPE AND DATES COVERED

4. TITLE AND SUBTITLE	5. FUNDING NUMBERS
INFLUENCE OF ADDED GRAPHITE ON THE MECHANICAL STRENGTH OF PRESSED PLASTIC BONDED EXPLOSIVES	

6. AUTHOR(S)

Donald A. Wiegand

7. PERFORMING ORGANIZATION NAME(S) AND ADDRESSES(S)	8. PERFORMING ORGANIZATION REPORT NUMBER
ARDEC, AED Energetic Warheads Division (AMSTA-AR-AEE-W) Picatinny Arsenal, NJ 07806-5000	

9.SPONSORING/MONITORING AGENCY NAME(S) AND ADDRESS(S)	10. SPONSORING/MONITORING AGENCY REPORT NUMBER
ARDEC, DOIM Information Research Center (AMSTA-AR-IMC) Picatinny Arsenal, NJ 07806-5000	Technical Report ARAED-TR-95018

11. SUPPLEMENTARY NOTES

12a. DISTRIBUTION/AVAILABILITY STATEMENT	12b. DISTRIBUTION CODE
Approved for public release; distribution is unlimited.	

13. ABSTRACT (Maximum 200 words)

Composite plastic bonded explosive samples containing 80% and 85% HMX (cyclotetramethylene tetranitramine) in a polymer-plastizer binder were produced by mixing, extruding, cutting, drying, and pressing. Before pressing, the extruded material was in some cases coated with a thin layer of graphite (≈ 1 μm) for ease in pressing. As part of a general study of these composites, the compressive strength was determined as a function of temperature, strain rate, and the amount of the graphite added. Without graphite, the compressive strength increases with decreasing temperature and increasing strain rate. With graphite, this strength has the same behavior above approximately -10°C, but is insensitive to both temperature and strain rate below this temperature for a strain rate of 1.0/sec. In addition, the low temperature value of the compressive strength appears to decrease with increasing graphite thickness. The cracking and fracture patterns are temperature and strain rate dependent and are different with and without graphite. These results indicate that the bond produced by pressing the graphite containing material is stronger than the composite above about -10°C and weaker below this temperature so that failure initiates in the composite above about -10°C and in the bond below -10°C. With increasing strain rate this transition temperature increases. The results also indicate that the bond produced by pressing the material without graphite is at least as strong as the extruded material itself.

14. SUBJECT TERMS	15. NUMBER OF PAGES 27
Composite Plastic bonded explosive Compressive strength Pressed Strain rate Temperature	16. PRICE CODE

17. SECURITY CLASSIFICATION OF REPORT UNCLASSIFIED	18. SECURITY CLASSIFICATION OF THIS PAGE UNCLASSIFIED	19. SECURITY CLASSIFICATION OF ABSTRACT UNCLASSIFIED	20. LIMITATION OF ABSTRACT SAR

ACKNOWLEDGMENTS

CONTENTS

FIGURES

INTRODUCTION

As part of a general study of the mechanical properties of pressed composite plastic bonded explosives, the strengths of two very similar pressed composites were investigated as a function of several parameters. The strength is of interest over the temperature range of -45°C to 65°C and over a strain rate range from <0.001 to >10/sec. However, the strength is of particular interest at the lower end of this temperature range because of a problem with cracking on thermal cycling.

To facilitate ease in pressing and in particular to alleviate a sticking problem, a thin graphite coating was added to the composite plastic bonded explosives before pressing. This graphite eliminated the sticking problem, but may have aggravated the low temperature cracking problem. In order to gain some understanding of the differences in the types of bonding which are produced during the pressing process in samples with and without graphite, the strength was investigated over the temperature and strain rate range and as a function of the amount of graphite added.

EXPERIMENTAL

The two composite plastic bonded explosives have slightly different compositions. The percentage of solid filler [high melt explosive (HMX)] was either 80% or 85%; the percentage of polymer [cellulose acetate butyrate (CAB)], was 8% or 6%; and the percentage of plastizer, [bis(2,2-dinitropropyl acetyl/formal (BDNPA/F)] was 12% or 9%. These two explosive formulations are PAX 2 (80% HMX) and PAX 2A (85% HMX), respectively. A HMX is an organic polycrystalline material with an average particle size of about 4 μm as used here. Composites were prepared and pressed either at Picatinny Arsenal (P), or prepared at Hercules (H) and pressed at Iowa Ammunition Plant (I), and are designated here as PAX 2 (P), PAX 2 (H/I), PAX 2A (P), and PAX 2A (H/I) to indicate the composite and the preparation and pressing locations.

Samples were prepared by mixing with a suitable solvent and extruding in cylinderical form at diameters of 0.127 cm (P) or 0.254 cm (H/I) [0.05 in. or 0.1 in.]. The material was then cut into cylinders with the length equal to the diameter and dried to eliminate the solvent (refs 1 through 3). For the work reported here, these small extrusion cylinders were then pressed at ambient temperature (P) or at about 57°C (135°F) (I) into cylinders of approximately 0.5 in. (P) or 0.75 in. (I) in diameter and length and of the desired density. However, somewhat higher densities were obtained at one of the locations (I). Porosities were generally between about 0.3% and 0.7%, but in some cases were as high as 1.3%. Because of the sticking problem during the pressing of larger quantities of these composites, the small extrusion cylinders were in most cases coated with a small amount of graphite, 0.06% to 0.19% by weight for the samples

considered here. The graphite coating was applied by placing the extrusion cylinders and the desired amount of graphite in a closed container (glaze barrel) and tumbling for several minutes until most of the graphite was coated onto the extrusion cylinders (refs 2 and 4). Cylinderical samples of graphite 0.25 in. in diameter and length were also pressed at ambient temperature to densities close to 1.45 gm/cm³ using the same graphite that was used for the coatings. Samples of graphite with the same diameter, but with several smaller lengths, were also pressed and measured.

All samples were uniaxially compressed at constant strain rate along the cylinder axis using an MTS servo-hydraulic system (ref 5). The composite samples without the graphite coating on the extrusion cylinders were coated with graphite on the flat cylinder ends to minimize friction during compression. Complete stress versus strain curves were recorded, but only the maximum compressive stress (i.e., the compressive strength) is reported here. Other results were presented (refs 6 and 7) and will be published separately (ref 8). Measurements were made as a function of temperature between -60°C and 65°C and as a function of strain rate between approximately 0.001/sec and 10/sec.

RESULTS

A typical curve of stress versus strain at higher temperatures is given in figure 1. The stress increases linearly with strain after the initial curvature, curves over and passes through a maximum, and then decreases for further increases of strain. At lower temperatures (where fracture is observed) the stress versus strain curve is similar to figure 1 up to the maximum stress, but there is an abrupt decrease of the stress to near zero at or just after the maximum. The maximum stress, the compressive strength, is used here as a measure of the stress for failure, i.e., yield and/or fracture. Yield and plastic flow like behavior are observed at higher temperatures and fracture at lower temperatures, and the transition between the two types of behavior is strain rate dependent.

In figure 2, the compressive strength is given as a function of temperature for samples of one of the composites with and without the graphite coating on the extrusion cylinders and for a strain rate of 10/sec. Similar data were obtained at other strain rates and for the other composite. The temperature dependence for the two types of material of figure 2 is similar above a transition temperature of about -10°C, but is strikingly different below this temperature. Thus, the graphite coating has a strong effect on the strength in the low temperature region and a much smaller effect in the high temperature region. The differences above -10°C may be due, at least in part, to differences in composition other than the graphite and also differences in density. In figure 3, the compressive strength is given as a function of temperature for the graphite containing material for a few strain rates. While the compressive strength increases with strain

rate over most of the temperature range, it is insensitive to strain rate at the lowest temperature. With decreasing temperature at any strain rate, the compressive strength increases until it reaches a value in the vicinity of 38 MPa (fig. 2) and then becomes insensitive to temperature for further decreases of temperature. As indicated in figure 3, this transition temperature increases with increasing strain rate. In figure 4, the compressive strength is given versus strain rate for two temperatures for samples with and without graphite. The two types of samples have the same strain rate dependence at 27°C, but quite different strain rate dependencies at -40°C. In general, the compressive strength increases with increasing strain rate and decreasing temperature at all temperatures and strain rates investigated for samples without graphite and for samples with graphite above the transition temperature. The latter is strain rate dependent a noted. Forthe material with graphite at and below the transition temperature, the compressive strength is insensitive to both temperature and strain rate.

In summary, the low temperature compressive strength of the graphite containing material is insensitive to temperature and strain rate within the range of measurements. However, the strength of the graphite containing material above the transition temperature and the strength of the material without graphite over most of the temperature range increased with decreasing temperature and increasing strain rate. The transition temperature for the onset of the plateau of compressive strength versus temperature in the graphite containing material (i.e., about -10°C for the data of figure 2) is strain rate dependent and at lower strain rates this onset occurs at lower temperatures (fig. 3).

In figure 5, the low temperature compressive strength at -40°/45°C (in the plateau region of figure 2) is plotted versus the average total thickness of the graphite layer between the extrusion cylinders. This thickness was estimated from the amount of graphite used and by assuming that the extrusion cylinders were uniformly coated. In each case with graphite, the plotted value was obtained by averaging the values for all strain rates since the results are insensitive to strain rate at these low temperatures (figs. 3 and 4). The error bars for the compressive strength give the standard deviations of the measured values used in the averaging. The value for PAX 2 (P) without graphite (zero thickness) was obtained by averaging the values for all strain rates except the lowest strain rate, and the standard deviation reflects the strain rate dependence shown in figure 4. For PAX 2A (P) without graphite, the results for all strain rates were used because the available data does not show a clear strain rate dependence. Data is not available for PAX 2(H/I) and PAX 2A(H/I) without graphite. The number of measurements varied from four to twenty for the different graphite thicknesses. The error bars for the average graphite thickness reflect the estimated uncertainties in the amount of graphite applied and so the average thickness. The data of figure 5 clearly indicates the decrease in the compressive strength associated with the presence of graphite (fig. 2) and further indicates a decreasing compressive strength with increasing graphite

layer thickness. The apparent structure of figure 5 (maximum at 0.566 μm) is due to variations other than the graphite content since this structure is also observed at 25°C, although the decrease of the compressive strength due to the presence of the graphite is much smaller at the higher temperature. When the compressive strengths at -40/-45°C are normalized to the values at 25°C, the structure is mostly eliminated. Both composites prepared at both locations are represented in figure 5, as indicated, and the apparent structure is most probably due to differences in the densities obtained at the two locations and possibly to differences between the two composites. As noted previously, the densities of samples pressed at I tend to be higher than the densities of samples pressed at P. While compressive strength versus density data is not available for the composites with graphite, the compressive strengths of samples of PAX 2A without graphite and samples of pressed graphite both increase with density. There-fore, the points of figure 5 for PAX 2 (H/I) and PAX 2A (H/I) may be high relative to the points for PAX 2 (P) and PAX 2A (P) because of density differences. Additional work is required to further resolve this question.

The condition of the samples after large deformations is also of interest. The results are temperature, and to some extent, strain rate dependent. At the high temper-ature extreme (i.e., at 65°C), all samples appear to have deformed plastically with little or no indication of external cracking but with significant barreling. At 25°C, samples with the graphite coating indicate both barreling and significant cracking; and the cracks are predominantly, if not completely, along the graphite boundaries between extrusion cylinders. Because the composite is white and the graphite is black, fracture at the graphite boundary can easily be distinguished visually from fracture in the composite. At 25°C, the samples without graphite also exhibit barreling and cracking, but the cracks do not appear to be predominantly between extrusion cylinders. At lower temperatures (primarily -10°C and -45°C) there is very significant fracture and fragmentation for samples with and without graphite. For the material without graphite, the shape and size of the fragments indicate that fracture did not take place predominantly along the boundaries between extrusion cylinders. For samples with graphite and having the thinner graphite layers (fig. 5), the same is true. However, as the thickness of the graphite layer increases, the fraction of the fracture surfaces which are graphite coated increases, thus indicating significant fracture at the graphite boundaries.

Because the graphite coating has such a marked effect on the temperature and strain rate dependence of the composites, the graphite used for the coatings was pressed into cylinders under approximately the same conditions as the composites and the compressive strength measured as a function of temperature and strain rate. The compressive strength of the graphite was found to be temperature and strain rate dependent and to increase with decreasing temperature and increasing strain rate, but to be significantly less sensitive to temperature and definitely less sensitive to strain

rate than the composites. While the loading conditions and so failure conditions for the graphite layers in the composite are different from those of the pressed pellets, these results do indicate that the strength of the graphite used in this work is much less temperature and strain rate sensitive than the composites.

The compressive strength of the pressed graphite samples with the length equal to the diameter is in the range of 1 to 5 MPa and so much lower than the low temperature values of about 35 to 60 MPa for the composites of figure 5. While the compressive strength of the graphite also increases with density, extrapolation of the limited available data as a function of density to graphite crystal density still gives a value significantly less than 35 MPa. However, the graphite in the composites is confined and studies with other materials indicate that the strength significantly increases with confinement (ref 9). In addition, studies with other materials indicate that the compressive strength increases when the ratio of the length (L) to the diameter (D), (L/D), of the samples decreases (refs 7 and10), and for one material the strength for small L/D was found to be equal to the confined value (refs 7 and 9). This occurs because for small L/D most of the sample is effectively confined (refs 7 and 11 through 13). Although measurements were not made on confined graphite, they were made as a function of L/D and the results indicate an increasing compressive strength with decreasing L/D as found for other materials. While the maximum observed compressive strength for the L/D measurements is still less than the lowest values found for the graphite containing samples of the composite at low temperatures, the L/D of the graphite in the composite is much less than the values easily attainable using graphite alone. The results to date then suggest that 35 to 60 MPa is the strength of the graphite at low temperatures for the confinement conditions of the composite (fig. 5). Additional work is necessary to further resolve this matter.

DISCUSSION

As noted previously, the stress as a function of strain for these composite plastic bonded explosives increases approximately linearly with increasing strain, curves over, and passes through a maximum, and then decreases toward zero stress with further increases in strain at higher temperatures (fig. 1), or decreases abruptly to near zero just after the maximum with increasing strain at lower temperatures. Failure is taken here to be due to whatever processes are responsible for this yield like behavior indicated by the deviation from linearity of the stress versus strain curve. The compressive strength is taken as a measure of the stress required for this yield like failure, although this behavior occurs at a somewhat lower stress. The apparent softening at larger strains is not considered here (ref 7).

There are several bonds to consider in addressing the failure of these materials. In all cases, there is the bond between the solid filler particles (HMX) and the polymer-plasticizer binder, i.e., failure could be due to dewetting. In addition, in the materials

without graphite there is the bond between the extrusion cylinders produced during pressing. And finally, in the materials with graphite there is a bond between the graphite coating and the composite and a graphite-graphite bond between the graphite coated extrusion cylinders. Failure may initiate in any one of these bonds, in the solid filler or in the polymer-plastizer.

The experimental results are consistent with the following descriptions of failure. For the material without graphite, failure occurs primarily in the bulk composite and not in the bonds between extrusion cylinders. The surfaces of the samples after pressing contain a mosaic like pattern associated with the extrusion cylinders and when crack and fracture lines are observed they do not primarily follow the boundaries of the extrusion cylinders as detected by this mosaic pattern. Thus, the strength of the bond produced by pressing must approach or exceed the strength of the bulk extruded material, i.e., the boundary is effectively eliminated in the pressing process. This is supported by measurements of individual extrusion cylinders at -45°C and 25°C which indicate compressive strengths comparable to the pressed samples. In addition, for samples produced by first grinding the extrusion cylinders to a powder and then pressing, the compressive strengths are comparable to the compressive strengths of the individual extrusion cylinders and to strengths of the samples produced by pressing the extrusion cylinders without grinding. This latter result indicates that significantly increasing the surface area of the bond produced by pressing does not influence the strength of this bond. The compressive strength of the pressed samples increases with increasing strain rate and decreasing temperature and at low temperatures fracture and fragmentation are observed while at higher temperatures a plastic flow like behavior is found. Both of these are as expected for a polymer-plastizer system, thus indicating that the polymer-plastizer plays a strong role in the failure processes.

For the graphite coated samples, the failure process in the high temperature region is the same as in the material without graphite because the graphite bonds are stronger than the composite. With decreasing temperature at any strain rate, the composite strength increases significantly while that of the graphite is insensitive to temperature. At some low temperature (depending on strain rate) the stress required to initiate failure in the graphite equals that of the composite. At lower temperatures, failure initiates primarily in the graphite because the composite is stronger than the graphite. Since the strength of the graphite is less sensitive to strain rate than the strength of the composite, the temperature at which the composite strength equals the graphite strength is strain rate dependent and increases with strain rate.

The observations of the sample conditions at large deformations are consistent with the failure descriptions just given. At 25°C and 65°C, failure apparently in the form of plastic flow occurs in the bulk material with and without graphite. With graphite, the distortion of the extrusion cylinders by plastic flow can generate stress concentrations in the graphite which eventually causes cracking and fracture in the graphite. Without the

6

graphite coating, the boundaries effectively do not exist because of the welding (bonding) which takes place on pressing so that this type of cracking/ fracture is not observed (ref 14). Because of the observed fracture pattern at lower temperatures where failure is thought to originate in the graphite in the form of crack generation, crack propagation in the graphite apparently can continue into the bulk when the moving crack meets the (blunt) side of an extrusion cylinder. The latter occurs in part because of the brittle nature of the bulk material at low temperatures.

The data for PAX 2 (P) of figures 2 and 5 clearly indicate a very significant decrease of the compressive strength with added graphite in the low temperature region. The results of figure 5 for PAX 2A (P) are not so obviously conclusive because of the nearly overlapping standard deviations. However, consideration of the temperature and strain rate dependencies in the low temperature region clearly indicates differences. While PAX 2A (P) with graphite is insensitive to temperature and strain rate as is PAX 2 (P) at low temperatures (figs. 2 through 4), both PAX 2 (P) and PAX 2A (P) without graphite exhibit temperature and strain rate dependencies in this same low temperature region as illustrated for PAX 2 (P) in figures 2 and 4. In particular, the data for PAX 2A (P) without graphite at the higher strain rate indicates that there is a maximum in the curve of compressive strength versus temperature at a temperature above -45°C (i.e., at about -25°C) and the compressive strength in the vicinity of this maximum is significatly greater than the value with graphite. The lower temperatures were chosen for figure 5 because data is not available for some of the other materials at the higher temperatures. A maximum in the low temperature region for PAX 2 (P) without graphite is suggested by the data of figure 2. Thus, by taking the temperature dependence into consideration in addition to the data of figure 5, the results clearly indicate a significant difference in the compressive strengths in the low temperature region between samples without and with graphite. When these maxima are considered, some of the apparent difference at low temperatures between PAX 2 (P) and PAX 2A (P) without graphite (fig. 5) is also removed.

The data of figure 5 also suggests that the low temperature compressive strength decreases with increasing graphite thickness for the four graphite thicknesses given, neglecting the points without graphite. A least squares fit of a straight line to the four points of figure 5 with graphite, yields a negative slope with a correlation coefficient of 0.345 (ref 15). In addition, the results for the same thicknesses at 25°C and 65°C give similar magnitudes of relative negative slopes and similar correlation coefficients. The apparent structure of figure 5 (e.g., the maximum at 0.566 μm) is an important reason for the small magnitude of the correlation coefficient and as noted above this same structure is also found at 25°C and it has the same effect on the correlation coefficient at this temperature. When the low temperature data is normalized to the data at 25°C at each graphite thickness the structure is minimized and the correlation coefficient increases to 0.728 but with a much smaller negative slope.

Therefore, the results indicate that in addition to the very pronounced decrease in the compressive strength at low temperatures due to added graphite, there is smaller decrease at all temperatures studied, the magnitude of which increases with increasing graphite thickness. Other possible contributors to this trend of figure 5 (i.e., the decrease in the compressive strength with increasing graphite thickness) include differences in composition (e.g. PAX 2 versus PAX 2A) and differences due to the different preparation conditions at P and H/I. However, the points for the P and H/I materials of figure 5 taken separately each indicate a decrease of the compressive strength with increasing graphite thickness. This appears to eliminate preparation conditions as the cause of the trend of figure 5 and further indicates that the differences between the P and H/I materials contribute to the apparent scatter (structure) of this figure and thus to the small value of the correlation coefficient obtained by fitting one straight line to all four points. It therefore seems that graphite thickness is the only consistent cause of the trend of the data of figure 5. Measurements on one of the composites prepared at only one of the locations as a function of the graphite thickness are desirable to more conclusively establish this dependence of the strength on graphite thickness.

The dependence on graphite thickness could be due to one or more of the following: a) non-uniform graphite layer thickness and/or penetration of the graphite into the binder (discussed next) results in some binder-binder bonding which decreases as the graphite layer thickness increases; and/or b) the strength decreases as the L/D of the graphite layer increases as discussed prevously for the much larger L/D of pressed graphite samples. However, it is important to note that the graphite is confined in the composite but not in the large L/D pressed samples.

Although hardness measurements have not been made, the nature of the materials suggests that the graphite is harder than the composite. Light rubbing of the composite on graphite powder is sufficient to cover the surface of the composite with a thin layer of graphite. On pressing the graphite can then penetrate the composite more than graphite penetrates itself. This difference in penetration is a factor in the differences in the strength of the graphite-composite and the graphite-graphite bonds (ref 14).

SUMMRY AND CONCLUSIONS

The compressive strength of samples containing the graphite coating is insensitive to temperature and strain rate below a transition temperature which is itself strain rate dependent and increases with increasing strain rate. Above this transition temperature the strength of the graphite containing materials increases with increasing strain rate and decreasing temperature. In contrast, the compressive strength of material without graphite increases with increasing strain rate and decreasing temperature over all of

the temperature range investigated. This temperature and strain rate dependence indicates the importance of the polymer plastizer properties in the failure processes. The data also indicates that the compressive strength of the graphite containing samples decreases with increasing graphite coating thickness.

Because the strength of pressed graphite is insensitive to temperature and strain rate, and because the strength of the graphite containing composite decreases with increasing graphite coating thickness, and finally because of the fracture patterns it is concluded that the strength of the composite with graphite below the transition temperature is determined by the graphite and that failure originates in the graphite. Above the transition temperature failure in the graphite containing composite occurs in the composite because the magnitude and dependence of the strength on temperature and strain rate are similar to the material without graphite. The transition occurs because the graphite is stronger than the composite above and weaker below the transition temperature. The strength of the graphite containing material is less than that of the material without graphite over the whole temperature range investigated, but is significantly less in most of the low temperature range below the transition temperature. It thus appears that the low temperature cracking problem is aggravated by the addition of the graphite because the stress required for fracture is decreased by the graphite. The decrease of the compressive strength at lower temperatures and the other phenomena reported here will occur in the temperature range of interest in any plastic bonded explosive which is graphite coated before pressing if it's strength exceeds the graphite strength in this same temperature range.

The strength of the bond produced by pressing the material without graphite is comparable in magnitude or greater than the extruded bulk strength of the composite because the strength of the pressed material is comparable to the strength of the individual extrusion cylinders, and because the fracture patterns of the pressed samples do not in most cases indicate significant fracture along the boundaries of the mosaic pattern formed by pressing the extrusion cylinders together. In contrast, in material with the graphite coating the fracture patterns often follow the boundaries of the mosaic pattern and so indicate extensive failure in the graphite-graphite or graphite-composite bonds.
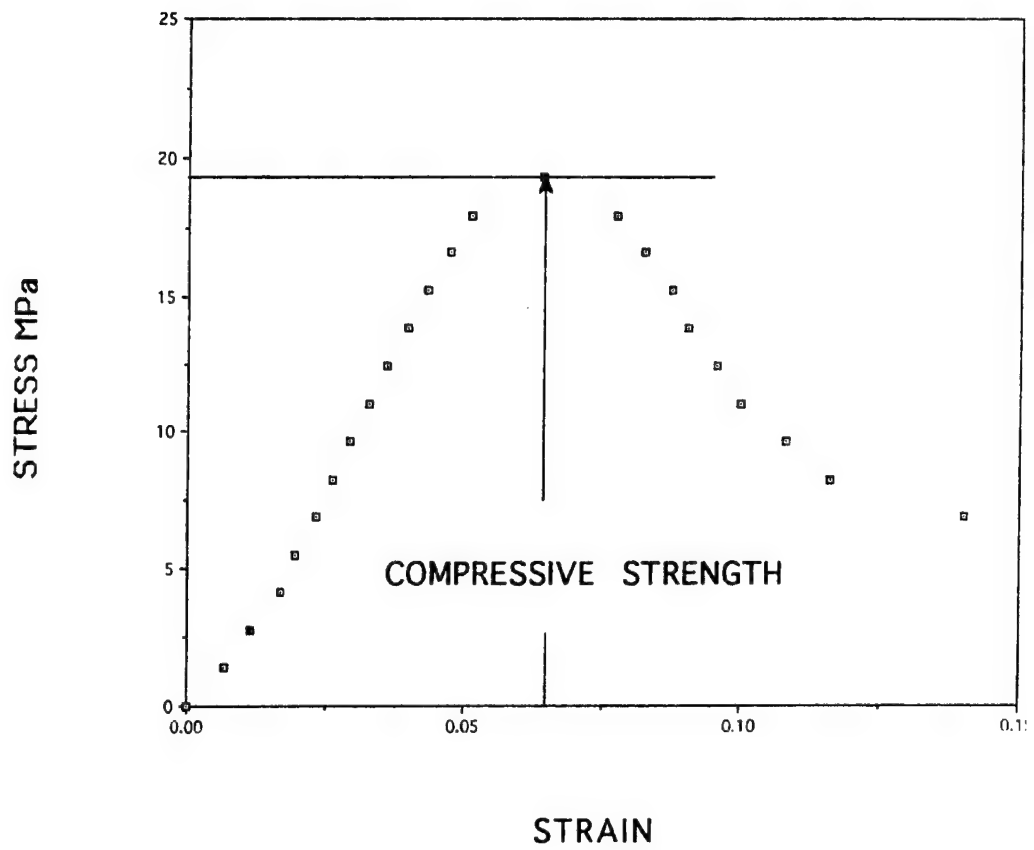
9

Figure 1
Typical stress versus strain curve in compression at higher
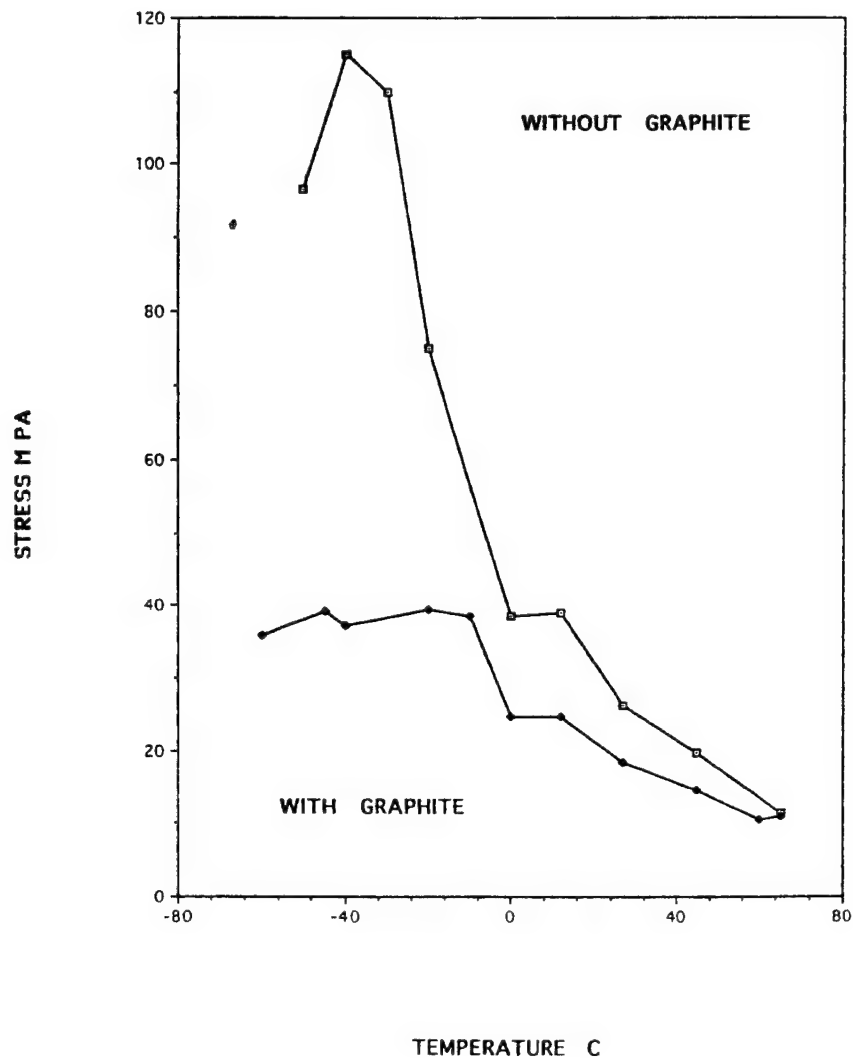temperatures [data for PAX 2A (P)]

Figure 2
Compressive strength versus temperature with and without graphite,
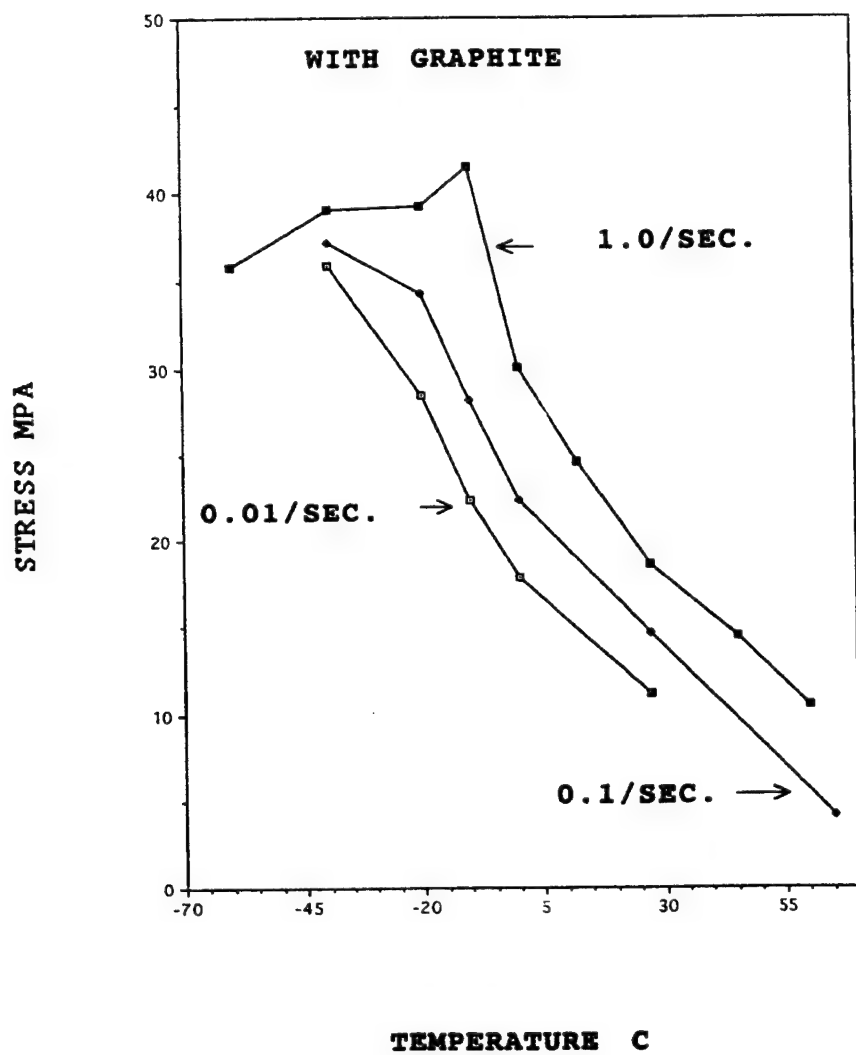strain rate 1.0/sec [data for PAX 2 (P)]

Figure 3
Compressive strength versus temperature for the graphite containing
material as a function of strain rate [data for PAX 2 (P)]
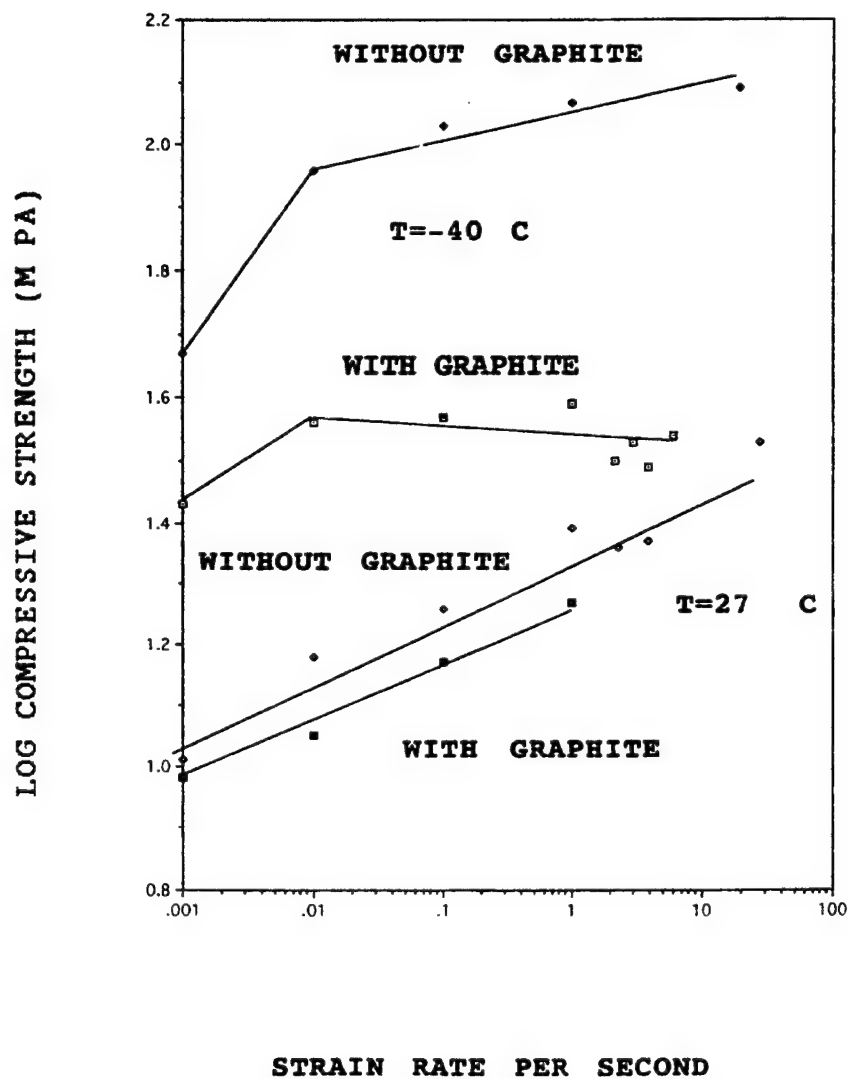
Figure 4
Logarithm of the compressive strength versus logarithm of the strain rate at -40°C
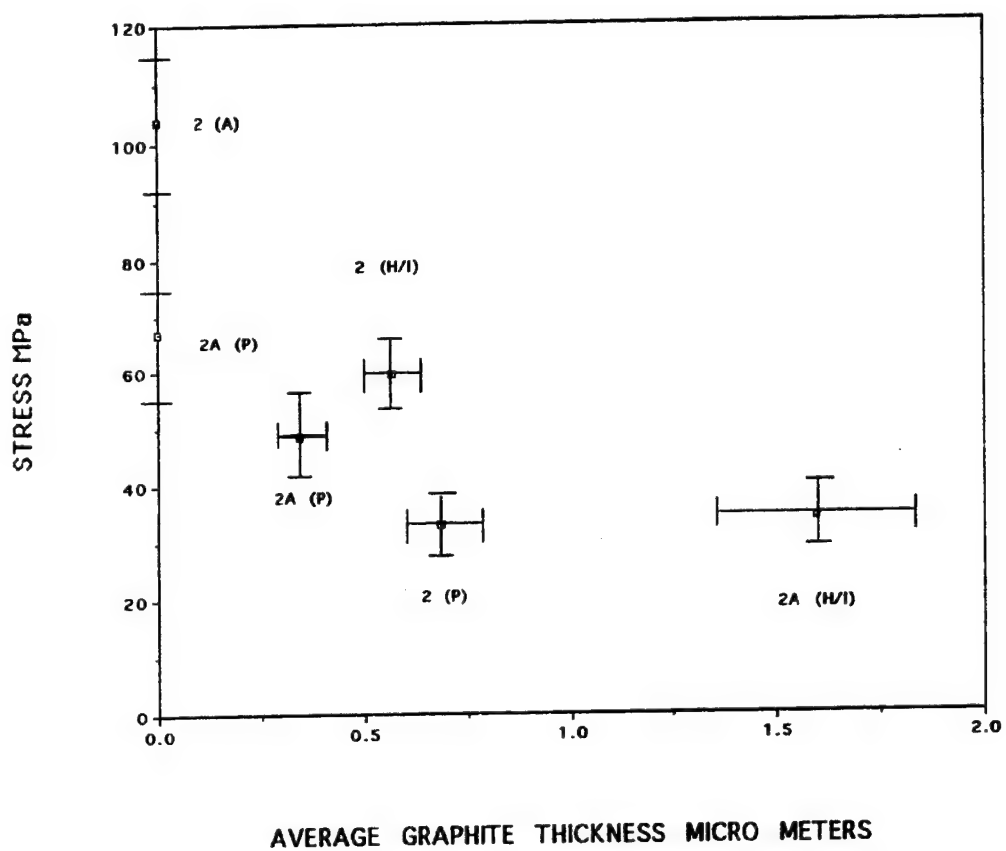and 27° C, with and without graphite [Data for PAX 2 (P)]

14

Figure 5
Low temperature (T = -40°/-45°C) compressive strength versus graphite
coating thickness, strain rate 1.0/sec

15

REFERENCES

1. Mezgar, M.; Strauss, B.; Moy, S.; and Prezelski, J., "Alternate Energetic Plastizers for Insensitive Explosive Compositions," U. S. Patent No. 4 842 659, 6 June 1989.

2. Strauss, B., Private Communication.

3. Wiegand, D. A., "Bond Strength of Pressed Composites," Materials Research Society Symposium Proceedings, Vol 318, Interfacial Control of Electrical, Chemical, and Mechanical Properties, Editors: S. P. Murarka, K. Rose, T. Ohmi and T. Seidel., p387, 1994.

4. Reppert, S., Private Communication.

5. Wiegand, D. A.; Pinto, J.; and Nicolaides, S., "The Mechanical Response of TNT and a Composite, Composition B, of TNT and RDX to Compressive Stress: I Uniaxial Stress and Fracture," J. Energetic Materials 9, 19, 1991.

6. Wiegand, D. A.; Hu, C.; Rupel, A.; and Pinto, J., "Fracture and Yield of Several Highly Filled Polymers," Proceedings of the 9th International Conference on Deformation, Yield and Fracture of Polymers, Churchill College, Cambridge, U.K., p 64, 1994.

7. Wiegand, D. A., "Critical Strain for Failure of Highly Filled Polymer Composites," Proceedings of the 3rd International Conference on Deformation and Fracture of Composites, University of Surrey, Guildford, U.K., p 558, 1995.

8. Wiegand, D. A., to be published.

9. Pinto, J. and Wiegand, D. A., "The Mechanical Response of TNT and a Composite, Composition B, of TNT and RDX to Compressive Stress: II Triaxial Stress and Yield," J. Energetic Materials 9, 205, 1991.

10. Hegemier, G. A. and Read, H. E., Prepared Discussion in Theoretical Foundations for Large-Scale Computations of Nonlinear Materials Behavior, Editors S. Nemat-Nasser, R. J. Asaro, and G. A. Hegemeir, Martinus Nijhopp, p 300, 1984.

11. Berglund, L. A. and Asp, L., "Fracture of Epoxies Subjected to Uniaxial and Triaxial Stress Fields," Presented at the 9th International Conference on Deformation, Yield and Fracture of Polymers, Churchill College, Cambridge ,U.K., 1994.

12. Gent, A. N. and Lindely, P. B., "Internal Rupture of Bonded Rubber Cylinders in Tension," Proc. Roy. Soc. (London), 249A, 195, 1959.

13. Lindely, G. H., "Traixial Fracture Studies," J. Appl. Phys, <u>38.</u> p 4843, 1967.

14. German, R. M., <u>Powder Metallurgy Science</u>, Metal Powder Industries Federation, Princeton, NJ, p.122, 1984.

15. Papoulis, A., <u>Probability, Random Variables and Stochastic Processes</u>, McGraw-Hill, NY, Second Edition, p 150, 1984.

DISTRIBUTION LIST

Commander
Armament Research, Development and Engineering Center
U.S. Army Tank-automotive and Armaments Command
ATTN: AMSTA-AR-IMC
             AMSTA-AR-GCL
             AMSTA-AEE-W, N. Slagg
             AMSTA-AEE-WW, B. Fishburn
                          M. Mezger
                          Y. Lanzerotti
                          D. Wiegand (15)
             AMSTA-AES
             AMSTA-AEE, J. Lannon
             AMSTA-AEE-B, D. Downs
                          S. B. Bernstein
             AMSTA-QAR-R, L. Manole
                          E. Bixon
             AMSTA-CCH-V, F. Hildebrant
             AMSTA-AEE-BR
             AMSTA-AET-M, R. Rupel
                          S. Cytron
Picatinny Arsenal, NJ 07806-5000

Commander
U.S. Army Production Base Modernization Agency
ATTN: AMSMC-PBM, A. E. Siklosi
                          D. Fair
Picatinny Arsenal, NJ 07806-5000

Defense Technical Information Center (DTIC)
ATTN: Accessions Division (12)
8725 John J. Kingman Road, Ste 0944
Fort Belvoir, VA 22060-6218

Director
U.S. Army Materiel Systems Analysis Activity
ATTN: AMXSY-MP
             AMXSY-D
Aberdeen Proving Ground, MD 21005-5066

Commander
Chemical/Biological Defense Agency
U.S. Army Armament, Munitions and Chemical Command
ATTN: AMSCB-CII, Library
Aberdeen Proving Ground, MD 21010-5423

Director
U.S. Army Edgewood Research, Development and Engineering Center
ATTN: SCBRD-RTB (Aerodynamics Technology Team)
Aberdeen Proving Ground, MD 21010-5423

Director
U.S. Army Research Laboratory
ATTN: AMSRL-OP-CI-B, Technical Library
         AMXBR-BLT, R. Frey
         AMXBR-BLC, J. Starkenberg
         AMXBR-TBT, R. Lieb
                   J. Rochehio
Aberdeen Proving Ground, MD 21005-5066

Chief
Benet Weapons Laboratory, CCAC
Armament Research, Development and Engineering Center
U.S. Army Armament, Munitions and Chemical Command
ATTN: SMCAR-CCB-TL
         SMCAR-LCB-RA, J. Vasilakis
Watervliet, NY 12189-5000

Director
U.S. Army TRADOC Analysis Command-WSMR
ATTN: ATRC-WSS-R
White Sands Missile Range, NM 88002

GIDEP Operations Center
P.O. Box 8000
Corona, CA 91718-8000

Office of the Secretary of Defense
OUSD(A)
Director, Live Fire Testing
Washington, DC 20301-3110

Director
U.S. Army Aviation Research and Technology Activity
Ames Research Center
Moffett Field, CA 94035-1099

Commander
U.S. Army Missile Command
ATTN: AMSMI-RD-CS-R (DOC)
Redstone Arsenal, AL 35898-5010

HQDA (SARD-TR)
Washington, DC 20310-0001

Commander
U.S. Army Tank-Automotive Command
ATTN: AMSTA-TSL (Technical Library)
Warren, MI 48397-5000

Commander
U.S. Army Materiel Command
ATTN: AMCDRA-ST
5001 Eisenhower Avenue
Alexandria, VA 22333-0001

Commander
U.S. Army Laboratory Commmand
ATTN: AMSLC-DL
Adelphi, MD 20783-1145

Commandant
U.S. Army Infantry School
ATTN: ATSH-CD-CSO-OR
Fort Benning, GA 31905-5660

Director
Armament Research, Development and Engineering Center
U.S. Army Tank-automotive and Armaments Command
Benet Weapons Laboratory
ATTN: AMSTA-CCB-TL
Watervliet, NY 12189-4050

Commander
U.S. Army Aviation Systems Command
ATTN: AMSAV-DACL
4300 Goodfellow Blvd.
St. Louis, MO 63120-1798

Commander
U.S. Army Research Office
ATTN: Chemistry Division
P.O. Box 12211
Research Triangle Park, NC 27709-2211

Commander
Naval Surface Warfare Center
ATTN: R10C, L. Roslund
         R10B, M. Stosz
         R13, J. Short
              R. Bernecker
              J. Forbes
Silver Spring, MD 20902-5000

Commander
Naval Weapons Center
ATTN: L. Smith
         A. Amster
         R. Reed, Jr.
China Lake, CA 93555

Commander
Ballastic Missile Defense Advanced Technology Center
ATTN: D. Sayles
P.O. Box 1500
Huntsville, AL 35807

Air Force Armament Technology Laboratory
ATTN: AFATL/DOIL
         AFATL/DLODL
Eglin AFB, FL 32542-5438

Southwest Research Institute
ATTN: M. Cowperthwaite
6220 Culebra Road
Postal Drawer 28510
San Antonio, TX 78284

New Mexico Institute of Mining and Technology
ATTN: TERA, T. Joyner
Campus Station
Socorro, NM 87801

Director
Lawrence Livermore National Laboratory
ATTN: R. McGuire
K. Scribner
M. S. Costantino
L-324
M. Finger
P.O. Box 808
Livermore, CA 94550

Director
Los Alamos National Laboratory
ATTN: J960, J. Ramsay
MS B221, J. Dienes
MS P952, J. Dick
P.O. Box 1663
Los Alamos, NM 87115

Southwest Research Institute
ATTN: H. J. Gryting
P.O. Box Drawer 28510
San Antonio, TX 78284

Honeywell, Inc.
ATTN: R. Tompkins
10400 Yellow Circle Drive
MN 38-330
Minnetonka, MN 55343

Commander
U.S. Army Armament, Munitions and Chemical Command
ATTN: AMSMC-ESM, W. D Fortune
AMSMC-IRD, G. H. Cowan
Rock Island, IL 61299-6000

Director
Sandia National Laboratory
ATTN: MS 432, J. Aidun
           MS 437, R. Thomas
           MS 477, T. Chen
Box 5800
Albuqure, NM

Johns Hopkins University
Applied Physics Laboratory
Chemical Propulsion Information Agency
ATTN: John Hannum
Johns Hopkins Road
Laurel, MD 20707

Morton Thiokol, Inc.
Louisiana Division
ATTN: Lee C. Estabrook
P.O. Box 30058
Shreveport, LA 71130

Commander
Naval Weapons Station
ATTN: L. Rothstein
           Code 50 - NEDED
Yorkstown, VA 23491